

TOPOLOGY AND CHIRAL SYMMETRY IN QCD WITH OVERLAP FERMIONS

ROBERT G. EDWARDS

*Jefferson Lab, 12000 Jefferson Avenue,
MS 12H2, Newport News, VA 23606, USA*

URS M. HELLER

*SCRI, Florida State University,
Tallahassee, FL 32306-4130, USA*

JOE KISKIS

*Dept. of Physics, University of California,
Davis, CA 95616*

AND

RAJAMANI NARAYANAN

*American Physical Society,
One Research Road, Ridge, NY 11961, USA*

Abstract. We briefly review¹ the overlap formalism for chiral gauge theories, the overlap Dirac operator for massless fermions and its connection to domain wall fermions. We describe properties of the overlap Dirac operator, and methods to implement it numerically. Finally, we give some examples of quenched calculations of chiral symmetry breaking and topology with overlap fermions.

1. Overlap formula for the chiral determinant

In the overlap formalism [1], the chiral determinant is obtained by embedding the Weyl fermion inside a Dirac fermion through a many-body problem. Let \mathcal{H}^\pm be two many-body Hamiltonians

$$\mathcal{H}^\pm = - \begin{pmatrix} a_1^\dagger & a_2^\dagger \end{pmatrix} H^\pm \begin{pmatrix} a_1 \\ a_2 \end{pmatrix}$$

¹Talk given by Urs M. Heller at the workshop "Lattice fermions and structure of the vacuum", October 5-9, 1999, xi Dubna, Russia.

$$H^- = \gamma_5 = \begin{pmatrix} 1 & 0 \\ 0 & -1 \end{pmatrix}; \quad H^+ = \gamma_5 (\gamma_\mu D_\mu - m) = \begin{pmatrix} -m & C(A) \\ C^\dagger(A) & m \end{pmatrix} \quad (1)$$

Let $|0\pm\rangle$ be the ground states of \mathcal{H}^\pm obtained by filling all the positive energy states of H^\pm . Then

$$\det C(A) \Leftrightarrow \langle 0- | 0+\rangle_A \quad (2)$$

“Proof”: $|0-\rangle$ is obtained by filling all the positive energy states of γ_5 , and $|0+\rangle$ by filling all the positive energy states of H^+ . They are of the form:

$$|0-\rangle : \begin{pmatrix} 1 \\ 0 \end{pmatrix}, \quad \text{and} \quad |0+\rangle : \frac{1}{N_k} \left(\begin{pmatrix} Cu_k \\ (\sqrt{\mu_k^2 + m^2} + m) u_k \end{pmatrix} \right), \quad (3)$$

where $C^\dagger Cu_k = \mu_k^2 u_k$ and N_k is the normalization.

The overlap formula is formal and needs to be regulated. It is valid only in the limit $m \rightarrow \infty$ and one should think of m as a pre-regulator. The formula is strictly valid only for ratios of determinants since there is a gauge field independent normalization in the formula.

H^+ need not have an equal number of positive and negative energy states and this happens for topologically non-trivial gauge fields, where the difference between the number of negative and positive energy states of H^+ is $2Q$. Then $\det C(A) = 0!$ Furthermore,

$$\langle 0- | a_{i_1}^\dagger \dots a_{i_Q}^\dagger | 0+\rangle \quad \text{or} \quad \langle 0- | a_{i_1} \dots a_{i_{|Q|}} | 0+\rangle \quad (4)$$

will be non-zero, for $Q > 0$ or $Q < 0$, respectively, resulting in fermion number violation. Potential anomalies reside in the phase of $|0+\rangle$. We will be concerned only with vector gauge theories, where only $|\langle 0- | 0+\rangle|^2$ enters and the anomaly is trivially cancelled in this case.

2. Lattice regularization

On the lattice $H^- \rightarrow H_L^- = \gamma_5$ remains unchanged, while

$$H^+ \rightarrow H_L^+ \equiv H_w(m) = \gamma_5 D_w(-m) = \begin{pmatrix} B(U) - m & C(U) \\ C^\dagger(U) & -B(U) + m \end{pmatrix} \quad (5)$$

where $C(U)$ is the naive lattice discretization of $C(A)$ and $B(U)$ is the standard Wilson term (with $r = 1$).

$|0-\rangle$ is still as in (3). Let $V = \begin{pmatrix} \alpha & \beta \\ \gamma & \delta \end{pmatrix}$ be the unitary matrix that diagonalizes H_L^+ , with the first and second “block-column” spanning the

subspaces of positive and negative eigenvalues, respectively. Then, for a vector theory,

$$|\langle 0 - | 0 + \rangle|^2 = \det \alpha \det \alpha^\dagger. \quad (6)$$

This can be obtained as the determinant of the overlap Dirac operator [2]

$$D_{\text{ov}} = \frac{1}{2} \left[1 + \gamma_5 \epsilon(\mathbf{H}_L^+) \right] \quad (7)$$

where $\epsilon(x)$ denotes the sign function. To see this consider,

$$D_{\text{ov}} V = \frac{1}{2} \left[\begin{pmatrix} \alpha & \beta \\ \gamma & \delta \end{pmatrix} + \gamma_5 \begin{pmatrix} \alpha & -\beta \\ \gamma & -\delta \end{pmatrix} \right] = \begin{pmatrix} \alpha & 0 \\ 0 & \delta \end{pmatrix}. \quad (8)$$

Since V is unitary we have $\det V = \det \delta / \det \alpha^\dagger$ and hence we obtain

$$\det D_{\text{ov}} = \det \alpha \det \alpha^\dagger. \quad (9)$$

The overlap Dirac operator can be generalized to the massive case

$$D_{\text{ov}}(\mu) = \frac{1}{2} \left[1 + \mu + (1 - \mu) \gamma_5 \epsilon(\mathbf{H}_L^+) \right] \quad (10)$$

where $-1 < \mu < 1$ is related to the fermion mass by [3]

$$m_f = Z_m^{-1} \mu (1 + \mathcal{O}(a^2)). \quad (11)$$

The propagator for external fermions is given by

$$\tilde{D}^{-1}(\mu) = (1 - \mu)^{-1} \left[D_{\text{ov}}^{-1}(\mu) - 1 \right], \quad (12)$$

i.e. it has a contact term subtracted, which makes the massless propagator chiral: $\{\tilde{D}^{-1}(0), \gamma_5\} = 0$.

A massless vector gauge theory can also be obtained from domain wall fermions [4], where an extra, fifth dimension, of infinite extent is introduced. In the version of ref. [5], one can show [6] that the physical (light) fermions contribute $\log \det D_{\text{DW}}$ to the effective action with the 4-d action

$$D_{\text{DW}} = \frac{1}{2} \left[1 + \mu + (1 - \mu) \gamma_5 \tanh \left(-\frac{L_s}{2} \log T \right) \right] \quad (13)$$

where T is the transfer matrix in the extra dimension and L_s its size. As long as $\log T \neq 0$ we obtain in the limit as $L_s \rightarrow \infty$

$$D_{\text{DW}} \rightarrow \frac{1}{2} \left[1 + \mu + (1 - \mu) \gamma_5 \epsilon(-\log T) \right]. \quad (14)$$

This is just the massive overlap Dirac operator up to the replacement $H_w \rightarrow -\log T$. It is easy to see that in the limit $a_s \rightarrow 0$, where a_s is the lattice spacing in the extra dimension (set to 1 above), one obtains $-\log T = H_w (1 + \mathcal{O}(a_s))$.

3. Some properties of the overlap Dirac operator

In many cases it is more convenient to use the hermitian version of the overlap Dirac operator (10):

$$H_o(\mu) = \gamma_5 D_{\text{ov}}(\mu) = \frac{1}{2} [(1 + \mu)\gamma_5 + (1 - \mu)\epsilon(H_w)]. \quad (15)$$

The massless version satisfies,

$$\{H_o(0), \gamma_5\} = 2H_o^2(0). \quad (16)$$

It follows that $[H_o^2(0), \gamma_5] = 0$, *i.e.* the eigenvectors of $H_o^2(0)$ can be chosen as chiral. Since

$$H_o^2(\mu) = (1 - \mu^2)H_o^2(0) + \mu^2 \quad (17)$$

this holds also for the massive case.

The only eigenvalues of $H_o(0)$ with chiral eigenvectors are 0 and ± 1 . Each eigenvalue $0 < \lambda^2 < 1$ of $H_o^2(0)$ is then doubly degenerate with opposite chirality eigenvectors. In this basis $H_o(\mu)$ and $D_{\text{ov}}(\mu)$ are block diagonal with 2×2 blocks, *e.g*

$$D_{\text{ov}}(\mu) : \begin{pmatrix} (1 - \mu)\lambda^2 + \mu & (1 - \mu)\lambda\sqrt{1 - \lambda^2} \\ -(1 - \mu)\lambda\sqrt{1 - \lambda^2} & (1 - \mu)\lambda^2 + \mu \end{pmatrix}, \quad (18)$$

where

$$\gamma_5 = \begin{pmatrix} 1 & 0 \\ 0 & -1 \end{pmatrix}. \quad (19)$$

For a gauge field with topological charge $Q \neq 0$, there are, in addition, $|Q|$ exact zero modes with chirality $\text{sign}(Q)$, paired with eigenvectors of opposite chirality and eigenvalue 1. These are also eigenvectors of $H_o(\mu)$ and $D_{\text{ov}}(\mu)$:

$$D_{\text{ov}}(\mu)_{\text{zero sector}} : \begin{pmatrix} \mu & 0 \\ 0 & 1 \end{pmatrix} \quad \text{or} \quad \begin{pmatrix} 1 & 0 \\ 0 & \mu \end{pmatrix} \quad (20)$$

depending on the sign of Q .

We remark that from eigenvalues/vectors of $H_o^2(0)$ those of both $H_o(\mu)$ and $D_{\text{ov}}(\mu)$ are easily obtained. There is no need for a non-hermitian eigenvalue/vector solver! For example, the Ritz algorithm [7] will do just fine.

4. Small eigenvalues and the chiral condensate

In the chiral eigenbasis of $H_o^2(0)$ the external propagator takes the block diagonal form with 2×2 blocks

$$\tilde{D}^{-1}(\mu) : \frac{1}{\lambda^2(1-\mu^2) + \mu^2} \begin{pmatrix} \mu(1-\lambda^2) & -\lambda\sqrt{1-\lambda^2} \\ \lambda\sqrt{1-\lambda^2} & \mu(1-\lambda^2) \end{pmatrix}, \quad (21)$$

and, in topologically non-trivial background fields the $|Q|$ additional blocks, depending on the sign of Q ,

$$\begin{pmatrix} \frac{1}{\mu} & 0 \\ 0 & 0 \end{pmatrix} \quad \text{or} \quad \begin{pmatrix} 0 & 0 \\ 0 & \frac{1}{\mu} \end{pmatrix}. \quad (22)$$

We thus find in a fixed gauge field background

$$\langle \bar{\psi}\psi \rangle(\{U\}) = \frac{|Q|}{\mu V} + \frac{1}{V} \sum_{\lambda>0} \frac{2\mu(1-\lambda^2)}{\lambda^2(1-\mu^2) + \mu^2}, \quad (23)$$

and averaged over gauge fields we get the condensate. It is dominated by the small (non-zero) eigenvalues and in the thermodynamic limit, where the first term vanishes, it is given by the density of eigenvalues at zero, $\rho(0^+)$.

With our normalizations we find for all chiral vectors $|b\rangle$

$$\mu \langle b | [\gamma_5 \tilde{D}^{-1}(\mu)]^2 | b \rangle = \langle b | \tilde{D}^{-1}(\mu) | b \rangle \quad \forall b \quad \text{with} \quad \gamma_5 | b \rangle = \pm | b \rangle. \quad (24)$$

This ensures the relation $\mu\chi_\pi = 2\langle \bar{\psi}\psi \rangle$ for every configuration, and, in fact, for every chiral random source used in a stochastic estimation of condensate and chiral susceptibility χ_π . For such stochastic estimates, we always work in the chiral sector with no zero-modes.

5. Implementations of the overlap Dirac operator

In practice, we only need the application of $D(\mu)$ on a vector, $D(\mu)\psi$, and therefore only the sign function applied to a vector, $\epsilon(H_w)\psi$. Since we need the sign function of an operator (a large sparse matrix) this is still a formidable task.

Methods proposed for this computation are:

- A Chebyshev approximation of $\epsilon(x) = \frac{x}{\sqrt{x^2}}$ over some interval $[\delta, 1]$ [8].
For small δ a large number of terms are needed.
- A fractional inverse method using Gegenbauer polynomials for $\frac{1}{\sqrt{x^2}}$ [9].
This has a poor convergence since these polynomials are not optimal in the Krylov space.

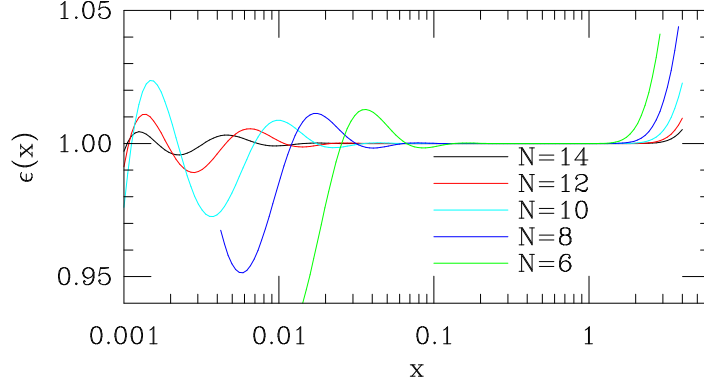


Figure 1. Plots of the optimal rational function approximation to $\epsilon(x)$ for various order polynomials.

- Use a Lanczos based method to compute $\frac{1}{\sqrt{x^2}}$ based on the sequence generated for the computation of $\frac{1}{x}$ [10].
- Use a rational polynomial approximation for $\epsilon(x)$ which can then be rewritten as a sum over poles:

$$\epsilon(x) \leftarrow x \frac{P(x^2)}{Q(x^2)} = x \left(c_0 + \sum_k \frac{c_k}{x^2 + b_k} \right) \quad (25)$$

The application of $\chi \leftarrow \epsilon(H_w)\psi$ can be done by the simultaneous solution of the shifted linear systems [11]

$$(H_w^2 + b_k)\phi_k = \psi, \quad \chi = H_w(c_0\psi + \sum_k c_k\phi_k). \quad (26)$$

One such approximation, based on the polar decomposition [12], was introduced in this context by Neuberger [13]. We use optimal rational polynomials [14]. The accuracy of this approximation is shown in Fig. 1.

We note that in all methods listed above, one can enforce the accuracy of the approximation of $\epsilon(x)$ for small x by projecting out the lowest few eigenvectors of H_w and adding their correct contribution exactly.

$$\epsilon(H_w) = \sum_{i=1}^n |\psi_i\rangle \epsilon(\lambda_i) \langle \psi_i| + \mathcal{P}_\perp^{(n)} \text{App}[\epsilon(H_w)] \mathcal{P}_\perp^{(n)}, \quad \mathcal{P}_\perp^{(n)} = \mathbf{1} - \sum_{i=1}^n |\psi_i\rangle \langle \psi_i|. \quad (27)$$

To invert $D^\dagger D$ for overlap fermions, we have, generically, an outer CG method (a 4-d Krylov space search) and an independent inner search

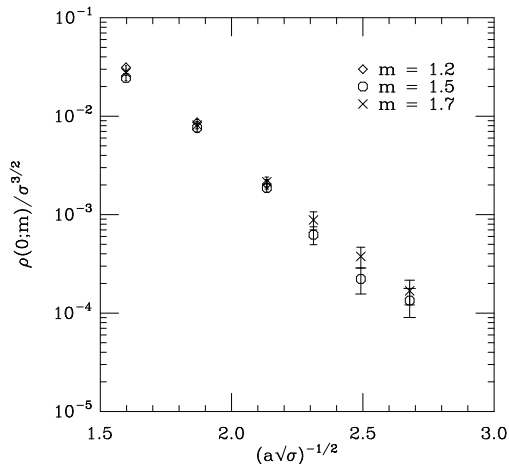


Figure 2. The approach of $\rho(0; m)$ to the continuum limit in the quenched theory.

method for $\epsilon(H_w)\psi$ – maybe CG again. For domain wall fermions, on the other hand, a 5-d Krylov space search method is used. It may pay off to try to combine inner and outer CGs for overlap fermions by reformulating them into a 5-d problem [15, 16].

6. Main problem for Overlap and Domain Wall fermions

For topology to change, we must create dislocations. These produce small modes which force the spectral gap of $H_w(m)$ to be closed. The density of zero eigenvalues of $H_w(m)$, $\rho(0; m)$, is non-zero in the quenched case, but rapidly decreasing with decreasing coupling [17]. Very roughly, we find $\rho(0; m)/\sigma^{3/2} \sim e^{-e^\beta}$ as shown in Fig. 2.

The existence of small eigenvalues hampers the approximation accuracy and convergence properties of implementations of $\epsilon(H_w)$. Eigenvector projection both increases the accuracy of the approximation and decreases the condition number, *e.g.* of the inner CG.

The existence of small eigenvalues has implications also for domain wall fermions. One can show that the spectrum of $-\log T(m)$ of Eq. (13) around zero is the same as the spectrum of $H_w(m)$ [1]. While the small eigenvalues of $-\log T(m)$ don't appear to cause algorithmic problems for domain wall fermions, they can induce rather strong L_s dependence of physical quantities, and causing hence the need for large L_s .

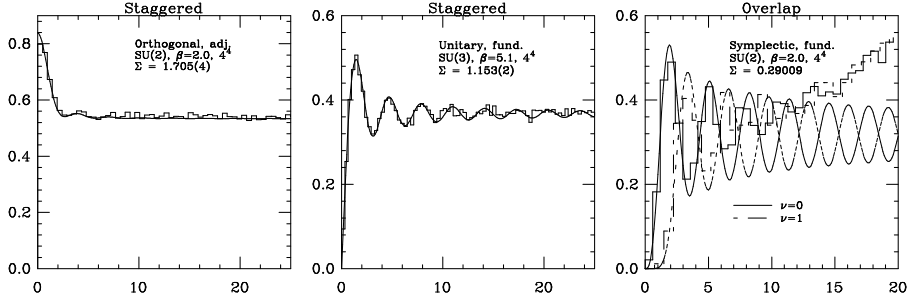


Figure 3. Examples for the microscopic spectral density for all three ensembles. For overlap fermions one can probe different topological sectors (rightmost panel).

7. The Dirac spectrum, chiral condensate and chiral Random Matrix Theory

Up to a scale, given by the infinite volume chiral condensate $\Sigma = \langle \bar{\psi}\psi \rangle$, RMT predicts that the rescaled density of eigenvalues

$$\rho_S(z) = \lim_{V \rightarrow \infty} \frac{1}{V} \rho \left(\frac{z}{V\Sigma} \right) \quad (28)$$

is universal, dependent only on the symmetry properties, number of dynamical flavors, and the number of exact zero modes (the topological sector), but not the form of the potential in the random matrix theory, or low energy effective Lagrangian [18]. There are three classes of random matrices determined by their symmetry properties: orthogonal, unitary, and symplectic.

In Fig. 3 we show examples of the microscopic spectral density for all three ensembles and compare to the analytic predictions from RMT. With overlap fermions we can probe topologically non-trivial sectors.

Similarly, there are predictions in each ensemble and topological sector for the distribution of the lowest eigenvalue. Examples for the quenched theory with overlap fermions are shown in Fig. 4. The Σ 's extracted from fits in different ν sectors for each ensemble are consistent [19].

RMT also gives predictions for the finite mass and volume dependence of the chiral condensate in the small mass large volume regime,

$$\frac{\Sigma_\nu(u)}{\Sigma} = 2u \int_0^\infty dz \frac{\rho_S(z)}{z^2 + u^2} + \frac{\nu}{u}, \quad (29)$$

with $u = \mu\Sigma V$. Particularly interesting is the behavior at small u :

$$\Sigma_0^{\text{GUE}}(u)/\Sigma \sim -u \log u, \quad \Sigma_0^{\text{GOE}}(u)/\Sigma \sim \frac{1}{2}(\pi - u), \quad \Sigma_{0,1}^{\text{GSE}}(u)/\Sigma \sim u \quad (30)$$

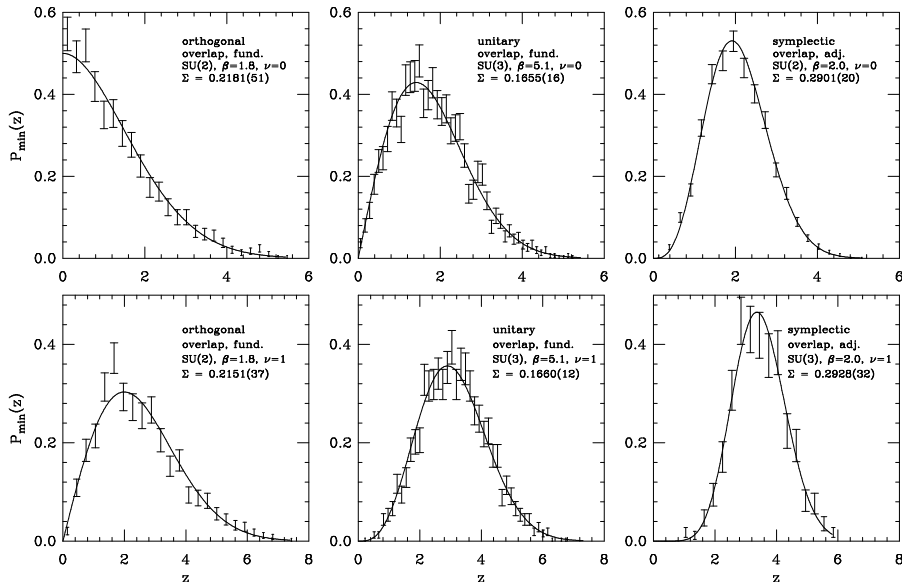


Figure 4. Plots of the distribution of the lowest eigenvalue for all three ensemble in the lowest two topological sectors. The curves are fits to the predictions from random matrix theory.

It is very sensitive to the lowest eigenvalues. In quenched QCD, surprisingly, $\Sigma_0^{\text{GOE}}(u)/\Sigma$ does not vanish at $u = 0$ in this microscopic limit. Our data, shown in Fig. 5 follow the predictions well [20]. Once again, with overlap fermions we can probe topologically non-trivial sectors. The finite volume corrections are quite large for overlap fermions: Σ is about a factor 7 smaller than in the staggered case. This implies that for overlap fermions larger volumes are needed to see the microscopic regime.

8. Small eigenvalue distribution in quenched QCD above T_c

We have studied the small eigenvalue distribution of the Dirac operator in the deconfined phase of quenched QCD. Sample distributions of small (non-zero) eigenvalues are shown in Fig. 6 [21].

For overlap fermions, we see the lower end of the bulk of the distribution, then a dip, or even a gap, and then again small eigenvalues, below about 0.05. We focus on the small modes, $\lambda < 0.05$. Our findings are summarized in Tables 1 and 2. We see that both $\langle n \rangle/V$ and $\langle Q^2 \rangle/V$ seem to remain finite and non-zero in the large volume limit for fixed β , but they drop

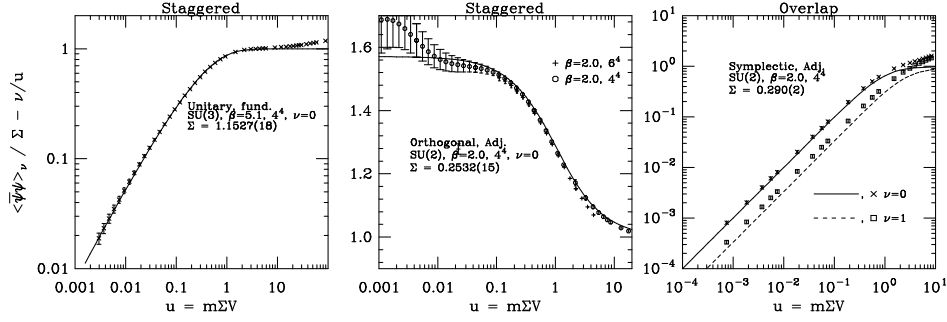


Figure 5. Examples of the behavior of the chiral condensate and the comparison to predictions from random matrix theory.

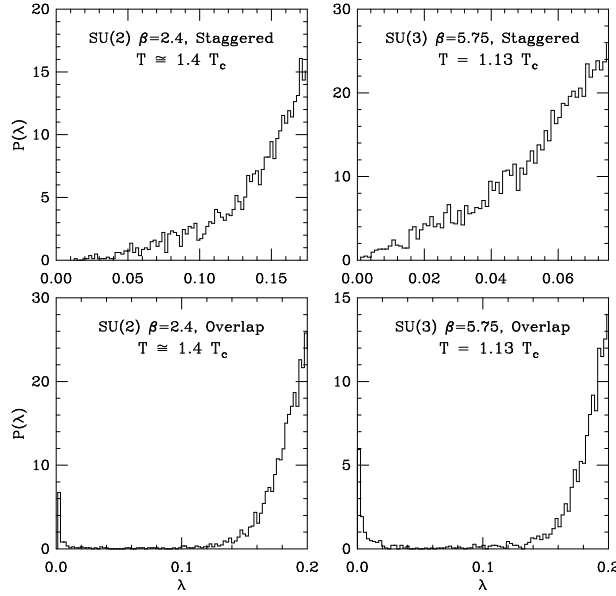


Figure 6. Low lying eigenvalue distributions in quenched QCD at finite temperature for staggered and overlap fermions.

quickly as β , and hence the temperature, is increased.

Looking in more detailed at the small modes we find

- Their number n is roughly Poisson distributed, $P(n, \langle n \rangle) = \langle n \rangle^n e^{-\langle n \rangle} / n!$. Average and variance are approximately equal.

TABLE 1. SU(3) data: $n = n_+ + n_-$ with n_{\pm} the number of zero and small non-zero eigenvalues with chirality \pm . $Q = n_+ - n_-$ is the topological charge. σ_n is the variance of n . The volume normalizations for n and Q^2 are per spatial 8^3 volume.

volume	$8^3 \times 4$		$12^3 \times 4$	$16^3 \times 4$		
β	5.75	5.85	5.75	5.71	5.75	5.85
$\langle n \rangle / V$	0.32	0.06	0.28	0.63	0.30	0.05
$\langle Q^2 \rangle / V$	0.31	0.07	0.28	0.64	0.33	0.05
$\langle n \rangle / \sigma_n$	1.09	0.90	0.92	1.15	1.03	0.83

TABLE 2. SU(2) data

volume	$8^3 \times 4$		$16^3 \times 4$	
β	2.3	2.4	2.4	2.5
$\langle n \rangle / V$	1.66	0.29	0.25	0.05
$\langle Q^2 \rangle / V$	1.66	0.31	0.25	0.05
$\langle n \rangle / \sigma_n$	0.97	1.09	0.93	0.99

– For fixed n , n_+ and n_- are roughly binomially distributed.

These observations are consistent with interpreting the small modes to be due to a dilute gas of instantons and anti-instantons, with n_+ and n_- their numbers. $n - |Q|$ of the would-be zero modes mix due to their overlapping and get small eigenvalues, while $|Q|$ exact zero modes remain.

At finite temperature, instantons fall off exponentially, and so do the fermionic zero modes associated with them. We consider a toy model of randomly (Poisson and binomially) distributed instantons and anti-instantons, inducing interactions of the form $h_0 e^{-d(i,j)/D}$ between the would-be zero modes of every instanton – anti-instanton pair (i, j) with separation $d(i, j)$. Like sign pairs are assumed to have no interactions. This toy model reproduces all qualitative features of the small eigenvalue distributions well for $D \approx 2$, corresponding to $D \approx 1/(2T)$ [21].

9. Conclusions

The overlap Dirac operator has the same chiral symmetries as continuum fermions. It has exact zero modes in topologically non-trivial gauge fields. It is therefore well suited for a study of the interplay of topology, with its

associated exact zero modes, and chiral symmetry breaking, determined by the density of small eigenvalues.

In the range of its validity the predictions of chiral random matrix theory are well followed and confirmed by overlap fermions, including the dependence on topology, given by the number of exact zero modes.

A study of the small eigenvalues in quenched QCD above the deconfining transition temperature, T_c , shows that topology, manifested by exact zero modes, persists. Furthermore, a finite density of small eigenvalues persists, and their properties are well described by attributing them to the would-be zero modes of a random dilute gas of instantons and anti-instantons.

Acknowledgements

The work of RGE and UMH has been supported in part by DOE contracts DE-FG05-85ER250000 and DE-FG05-96ER40979.

References

1. R. Narayanan and H. Neuberger, *Nucl. Phys.* **B443** (1995) 305.
2. H. Neuberger, *Phys. Lett.* **B417** (1998) 141.
3. R.G. Edwards, U.M. Heller and R. Narayanan, *Phys. Rev.* **D59** (1999) 094510.
4. D.B. Kaplan, *Phys. Lett.* **B288** (1992) 342.
5. Y. Shamir, *Nucl. Phys.* **B406** (1993) 90; V. Furman and Y. Shamir, *Nucl. Phys.* **B439** (1995) 54.
6. H. Neuberger, *Phys. Rev.* **D57** (1998) 5417.
7. B. Bunk, K. Jansen, M. Lüscher and H. Simma, DESY-Report (September 1994); T. Kalkreuter and H. Simma, *Comput. Phys. Commun.* **93** (1996) 33.
8. P. Hernandez, K. Jansen, L. Lellouch, hep-lat/9907022.
9. B. Bunk, *Nucl. Phys. Proc. Suppl.* **B63** (1998) 952.
10. A. Borici, *Phys. Lett.* **B453** (1999) 46; hep-lat/9910045.
11. A. Frommer, S. Güsken, T. Lippert, B. Nöckel, K. Schilling, *Int. J. Mod. Phys.* **C6** (1995) 627; B. Jegerlehner, hep-lat/9612014.
12. N.J. Higham, Linear Algebra and Appl., Proceedings of ILAS Conference “Pure and Applied Linear Algebra: The New Generation,” Pensacola, March 1993.
13. H. Neuberger, *Phys. Rev. Lett.* **81** (1998) 4060.
14. R.G. Edwards, U.M. Heller and R. Narayanan, *Nucl. Phys.* **B540** (1999) 457; *Parallel Computing* **25** (1999) 1395.
15. H. Neuberger, hep-lat/9909043.
16. A. Borici, hep-lat/9909057.
17. R.G. Edwards, U.M. Heller and R. Narayanan, *Phys. Rev.* **D60** (1999) 034502.
18. For a recent review, see J.J.M. Verbaarschot, hep-ph/9902394.
19. R.G. Edwards, U.M. Heller J. Kiskis and R. Narayanan, *Phys. Rev. Lett.* **80** (1999) 4188.
20. P.H. Damgaard, R.G. Edwards, U.M. Heller and R. Narayanan, hep-lat/9907016.
21. R.G. Edwards, U.M. Heller, J. Kiskis and R. Narayanan, hep-lat/9910041.